Scan-to-BIM: Edge-driven Pipeline to Facade Reconstruction

Queruel Maxime[1,2], Bornhofen Stefan[2], Martin Pierre[1], Histace Aymeric[2]

[1]Bouygues Construction - Research and Development Innovation Department
[2]ETIS, UMR 8051, CY Cergy Paris Université, ENSEA, CNRS, F-95000

m.queruel@bouygues-construction.com

Abstract -
This paper presents a facade-level Scan-to-BIM pipeline from terrestrial laser scanning (TLS) data for energy renovation applications. The workflow combines image-based edge extraction, geometric processing, and procedural BIM modeling. A Point Cloud Edge (PCE) module extracts facade contours from panoramic TLS projections, which are then processed through plane detection, clustering, and line fitting to recover facade structures and openings. These elements are finally converted into IFC-compliant wall and opening entities using a Constructive Solid Geometry (CSG) scheme. Design to be fully automated, at this stage, the method remains semi-automated: building isolation is still conceptual and not yet implemented in the operational workflow, and the number of facade planes is specified by the user before reconstruction.

The pipeline is evaluated on both synthetic and real-world datasets. Synthetic experiments enable controlled analysis of the reconstruction stages, while real TLS data highlight the influence of edge quality and facade complexity. Results show that geometric reconstruction is robust when extracted edges preserve a clear structural hierarchy, but automatic edge extraction remains a major bottleneck on complex facades. The contribution of this work lies in integrating panoramic edge extraction, interpretable geometric reconstruction, and CSG-based IFC generation into a coherent facade-oriented Scan-to-BIM workflow.

Keywords -
Point Cloud, Laser Scanning, Scan-to-BIM, Edge Detection, Constructive Solid Geometry, IFC Modeling

1 Introduction

The construction sector is being reshaped by the energy transition, with the renovation of existing buildings playing a key role in reducing carbon emissions and improving energy performance. Measures such as thermal insulation, facade rehabilitation, and structural reinforcement require accurate, up-to-date information on existing structures. In this context, Building Information Modeling (BIM) provides an efficient framework for centralizing and managing renovation data. However, usable BIM models of existing buildings are often unavailable or outdated, particularly for older buildings whose original plans are missing or no longer match current conditions. As a result, producing reliable as-built digital models remains a major bottleneck in the digitization of renovation workflows. Scan-to-BIM addresses this issue by reconstructing BIM models from 3D capture data, typically acquired through laser scanning or photogrammetry. Although these techniques produce dense point clouds, sometimes enriched with color and texture, converting them into structured BIM elements still requires costly and time-consuming manual work, which limits the scalability of Scan-to-BIM in industrial renovation. This challenge has motivated increasing efforts toward automation. Recent advances in computer vision and artificial intelligence have improved the interpretation of unstructured 3D data, but fully reliable and semantically consistent Scan-to-BIM workflows remain difficult to achieve, particularly for existing facades.

Against this background, this study focuses on facade-level modeling for social housing and proposes a multi-stage, semi-automated Scan-to-BIM pipeline that transforms TLS point-cloud data into BIM-ready facade models. Its contribution lies in integrating established components into a coherent and complete facade-oriented workflow. More specifically, the study makes four contributions: (1) a reconstruction pipeline combining panoramic point-cloud edge extraction, geometric reconstruction, and CSG-based IFC generation, (2) a hybrid strategy that couples learned edge extraction with interpretable geometric reasoning for BIM-oriented facade modeling, (3) a clear distinction between the conceptual pipeline and the currently validated operational workflow and (4) an evaluation of the geometric core on synthetic data, together with an analysis of workflow behavior on real TLS facades.

The following sections review related work, describe the proposed method, and position it with respect to representative facade reconstruction and Scan-to-BIM approache

2 State-of-the-Art

The Scan-to-BIM process aims to generate semantically rich BIM models from 3D capture data. Its main stages generally include acquisition and registration, pre-processing, segmentation, and modeling, while automation and semantic quality remain major challenges [1, 2, 3]. Although acquisition technologies such as terrestrial laser scanning (TLS) and photogrammetry have

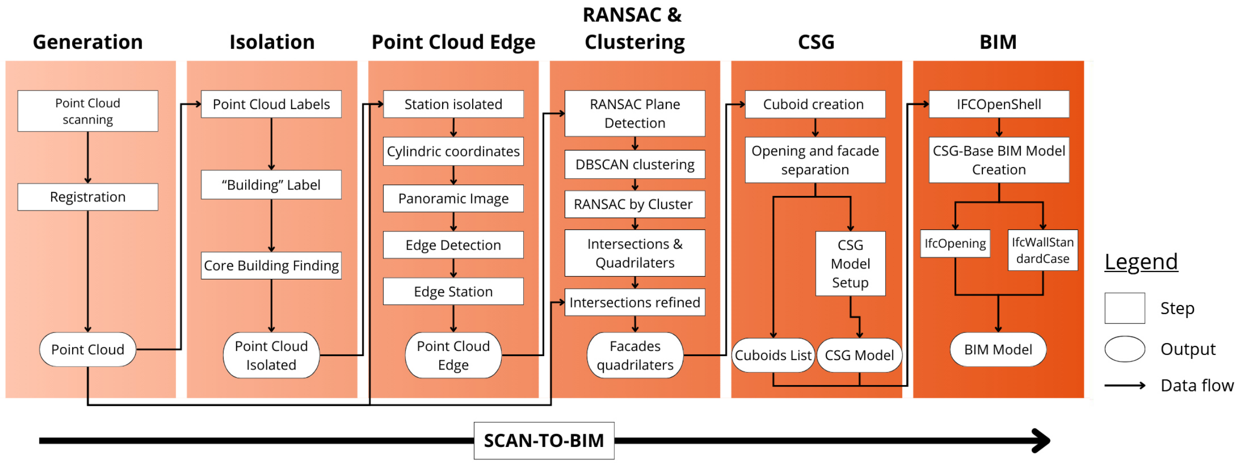

Figure 1. Overview of the full conceptual Scan-to-BIM pipeline applied to facades

reached industrial maturity, converting raw geometry into semantically structured BIM elements is still largely manual [4, 5]. This limitation highlights the need for more automated approaches that combine computer vision, machine learning, and BIM standards to produce consistent, usable models.

Recent progress in 3D deep learning has significantly improved point-cloud segmentation and classification. Architectures such as PointNet [6] and DGCNN [7] extract geometric features more robustly than traditional methods such as RANSAC or clustering [8, 9]. However, these approaches rely on large, annotated datasets, which remain scarce in the AEC domain. To address this limitation, hybrid methods combine deterministic geometry with data-driven learning, for example through RANSAC-based fitting enhanced by learned constraints [10, 11]. Such combinations improve robustness and generalization and provide an important basis for the proposed workflow.

For facade reconstruction, LiDAR and photogrammetry offer complementary strengths, with edge detection playing a central role in identifying structural boundaries. Traditional filters such as Sobel and Canny remain widely used but are highly sensitive to noise and surface texture. Deep learning-based detectors, including DexiNed [12] and TEED [13], outperform classical methods by producing finer, more continuous edges. Trained on dedicated datasets such as BIPED, these multi-scale convolutional networks also show strong cross-domain generalization. This robustness makes them particularly suitable for 2D-3D transposition, where edges extracted from panoramic images are reprojected into 3D point clouds [14, 15].

Facade modeling has evolved from manual reconstruction to procedural and parametric approaches. Early works based on shape grammars and hierarchical decomposition enabled the automatic detection of facade regularities from single images [16, 17]. In heritage contexts, semi-automatic procedural modeling has demonstrated the feasibility of linking rule-based facade generation with IFC entities [18]. Subsequent research has incorporated Constructive Solid Geometry (CSG) operations directly into IFC representations, allowing geometric primitives to be converted into BIM objects [19]. More recent hybrid methods combining geometric detection (Hough, RANSAC) and deep learning have shown promising results for facade reconstruction from point clouds [20, 11].

Recent studies have addressed complementary aspects of this problem. Boudarbala et al. detect doors and windows for as-built BIM by combining geometric and radiometric information [21]. Hu et al. extract facade structures through a semantic image laser point-cloud model with morphology-based optimization [22]. Ning et al. reconstruct wall facades with openings using occlusion handling, feature-line extraction, and graph-cut-based partitioning [20]. Bohórquez et al. propose a semi-automated parametric slicing workflow for facade retrofitting and IFC-oriented contour generation [23]. Overall, existing studies address learning-based segmentation, panoramic image generation from point clouds, facade parsing, geometric fitting, or IFC-oriented modeling, often as separate tasks or toward different reconstruction objectives.

In contrast, the present work focuses on their coordinated use within a facade-oriented Scan-to-BIM workflow whose target output is an IFC-compatible facade model. The contribution is therefore not a claim of novelty for each algorithmic block taken separately, but a methodological contribution at the workflow level: the integration of panoramic edge extraction, interpretable geometric reconstruction, and CSG-based BIM generation into a consistent reconstruction chain, together with an explicit analysis of its current operating conditions and failure cases on real TLS facades.

3 Scan-to-BIM pipeline

A facade reconstruction workflow was designed from TLS point clouds (see Figure 1). Its validated operational core comprises four stages: panoramic edge extraction, geometric reconstruction of facade, CSG translation and BIM generation. The automatic building isolation stage belongs to the full conceptual pipeline but is not yet part of the validated automated workflow reported in this paper.

3.1 Generation

The first stage consists of acquiring the point cloud using TLS, which is preferred to mobile (MLS) or airborne (ALS) systems. This choice is critical for achieving the geometric accuracy required for facade reconstruction, as TLS provides higher measurement precision and well-defined static stations, both essential for the panoramic projections used later. Photogrammetric images are also used to colorize the point cloud for subsequent processing. As is common in industrial workflows, the individual scans are pre-registered and merged into a single global point cloud using the manufacturer's software. The resulting dataset is stored in E57 format, which preserves both XYZ coordinates and acquisition metadata.

3.2 Isolation

In the full conceptual pipeline, this stage is intended to isolate the target building from its surroundings. It relies on point-cloud segmentation using deep learning models such as PointNet or DGCNN to classify points into two categories: Building and Environment. The points labeled as building are then grouped through clustering to distinguish individual structures, and the largest cluster is selected as the main building. Because the workflow focuses exclusively on external facades, interior points captured during scanning are removed. In the present study, however, this stage remains conceptual and is not implemented in the operational workflow. Building isolation is currently performed manually before reconstruction and is therefore not part of the validated automated pipeline reported in this paper.

3.3 Point Cloud Edge

The third stage consists of pre-processing the point cloud with the Point Cloud Edge (PCE) module, a hybrid approach that combines image-space analysis and spatial reprojection. In this framework, learned edge maps replace traditional geometric filters to improve precision while reducing complexity.

The input point cloud is first separated by acquisition station, and each station is processed individually to generate a panoramic image. A cylindrical projection is then used to map the 3D points onto a 2D plane. The panoramic image is generated from the full point cloud, since it includes both the building and the surrounding context required for reconstruction. Its resolution is set to 3144×1572, in line with prior recommendations that panoramic images should have a width approximately twice their height [14].

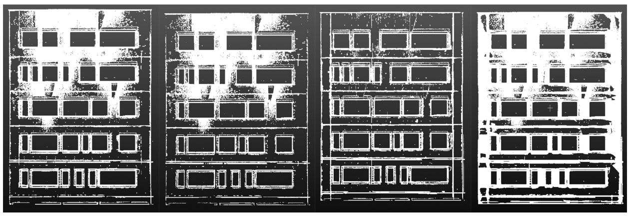

Figure 2. Visual difference of filter (from left to right) : Sobel, Canny, TEED, DEXINED

An edge detection algorithm is then applied to the panoramic images. Four methods were evaluated, including two traditional approaches (Sobel, Canny) and two deep-learning-based approaches (DexiNED, TEED). The quantitative results are reported in Table 3, and representative visual outputs are presented in Figure 2.

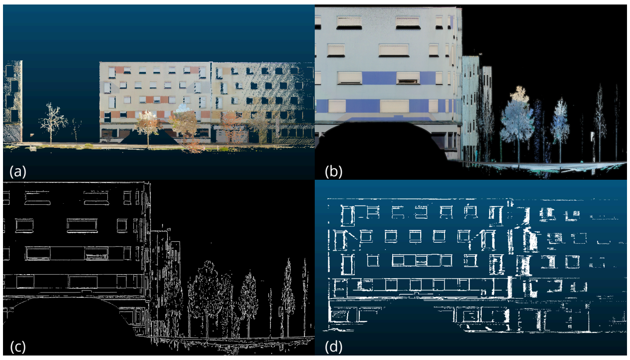

Figure 3. Example of PCE process : (a) Inital Point Cloud, (b) Panoramic Projection, (c) TEED filter, (d) Point Cloud Edge

Pixels detected as edges are preserved and projected back into 3D through inverse cylindrical mapping. Because only facade information is required, reprojection is applied to the isolated building point cloud, while points within the scanner's occlusion cone are removed to reduce noise. This process is repeated for each station, and the resulting edge-based point clouds are merged to retain complementary observations from different viewpoints and heights. However, projection and reprojection may introduce geometric uncertainty due to image discretization, point-cloud density, occlusions, non-uniform sampling, and viewpoint-dependent visibility. The resulting edge cloud should therefore be regarded as an approximation of the original 3D contour structure rather than a lossless transformation. In this study, this source of error is not quantified separately from other uncertainties in the pipeline, such as edge detection and geometric fitting.

3.4 RANSAC and Clustering

The next step extracts the structural elements of each facade. Since the PCE stage produces contour points and facade geometry can be approximated by parallelepiped shapes, the problem is reduced to sets of line segments in a local 2D frame. The point cloud is processed facade by facade, with the main planes detected using RANSAC. At this stage, the user manually specifies the number of facades to extract. For each detected facade, the inlier points are projected into a 2D coordinate system defined by Principal Component Analysis. In this 2D space, DBSCAN clusters the contour points into coherent groups corresponding to facade components. Within each cluster, a second RANSAC detects line segments constrained to be approximately horizontal or vertical in the facade frame. Their intersections are then computed to identify up to four corners forming a rectangular opening when the geometry is sufficiently orthogonal and consistent with the cluster structure. The detected corners are reprojected into 3D, where a local refinement is performed by retrieving neighboring points from the full scan, fitting a small local surface, and snapping the corner onto this surface when the adjustment is reliable; otherwise, the initial position is retained. The resulting quadrilaterals are finally classified into two categories: facade boundaries and opening contours.

3.5 CSG

Constructive Solid Geometry (CSG) is subsequently introduced for facade modeling [18, 19]. This approach describes a facade as a composition of simple geometric primitives whose combination produces the final shape. Two operations are used: DIFFERENCE and UNION. DIFFERENCE removes the volume corresponding to the openings from the wall, while UNION combines all remaining elements through a recursive process. This representation allows the facade to be expressed in a clear and structured manner and ensures full compatibility with BIM standards since each geometric operation directly maps to an IFC entity or operator.

3.6 BIM

The final step is BIM reconstruction. Using the CSG framework, the creation of BIM elements is directly associated with IFC operators. Through the recursive CSG process, the DIFFERENCE operator triggers the creation of an IfcOpening applied to a wall geometry, while the UNION operator merges all facades into a single IFC model. Some attributes of each element are also defined, such as its location, surface area (with or without openings for walls), and element name. The BIM reconstruction process includes two methods for modeling openings, based on two IfcOpening profile definitions: IfcRectangleProfileDef and IfcArbitraryClosedProfileDef. The first generates an opening using a bounding rectangle that fully contains the detected shape, whereas the second follows the exact geometry obtained from the clustering stage. The rectangular profile is suitable for quick estimations of facade surface areas, while the arbitrary profile provides a more accurate representation of the as-built condition.

4 Implementation and results

The proposed pipeline is evaluated on both synthetic and real-world TLS datasets. Synthetic data are first used to analyze the behavior of the geometric reconstruction stages under controlled conditions, providing a reference baseline independent of edge extraction quality. Real-world data are then used for a preliminary assessment of the approach on actual facades and to identify its current limitations under automatic PCE.

4.1 Input datasets

The synthetic dataset is generated from an IFC facade model using an open-source IFC-to-point-cloud generator [24]. The geometry is uniformly sampled to produce a noise-free point cloud, along with two noisy variants generated by adding Gaussian perturbations of 5 mm and 10 mm, representative of typical TLS acquisition noise. In this setting, ground-truth edge information is derived directly from the IFC geometry, allowing the geometric reconstruction pipeline to be evaluated independently of the PCE module.

The real-world datasets consist of two facades acquired with a Leica BLK360 TLS: an office building in Lille and a hospital facade in Argenteuil. All datasets were captured under the same acquisition protocol, using multiple static stations positioned outside the buildings and through windows to ensure sufficient viewpoint overlap. The scans were then registered into global E57 point clouds using the manufacturer's software.

For each real facade, a set of window corner points was manually annotated as ground truth for quantitative evaluation. These annotations are used to compare the behavior of the geometric reconstruction when driven by manually curated versus automatic PCE extraction. The real-world validation remains intentionally limited in scope and should be interpreted as preliminary. The two facades are used to examine the method under contrasting conditions, rather than to support broad claims of robustness or generalizability.

4.2 Evaluation methods

The first evaluation focuses on the geometric reconstruction block, which is identical across all experiments and tested on both synthetic data and real datasets using either ground-truth or automatic PCE, allowing geometric robustness to be distinguished from edge extraction quality. The second examines the behavior of the PCE module on real-world data, with particular attention to contour preservation and robustness to noise and occlusions. Performance is assessed using standard quantitative metrics, including precision and recall, Chamfer and Hausdorff distances, point-to-point errors, and opening-level measures based on true positives, false positives, false negatives, and mean Intersection-over-Union (mIoU).

4.3 Synthetic facade results

The geometric reconstruction pipeline was first evaluated on the three synthetic datasets described above. Because perfect ground-truth edges are available, these experiments provide an upper bound on the performance of the reconstruction stage under ideal conditions. Reconstructed openings are compared with the IFC reference using point-wise precision, Chamfer and Hausdorff distances, mean and median point-to-point errors, and mIoU between reconstructed and reference masks; the quantitative results are reported in Table 2.

Across all datasets, the pipeline achieves perfect precision (1.0) and an mIoU above 0.98, indicating correct detection of all openings and strong consistency between reconstructed shapes and the IFC reference. As noise increases, Chamfer and Hausdorff distances also increase, with the latter being especially sensitive to isolated extreme deviations. Despite these perturbations, the mean reconstruction error remains within a few centimeters,

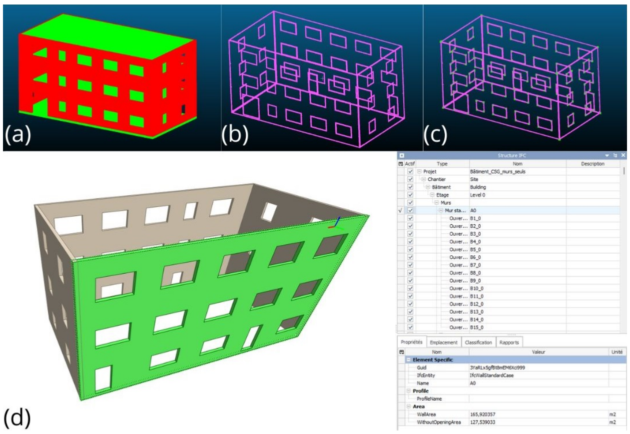

Figure 4. Process apply to Synth2 : (a) Synthetic Point Cloud, (b) Manual PCE results, (c) Detected intersections, (d) BIM results

which is acceptable for facade-scale renovation scenarios. From a practical BIM perspective, these results suggest that, under controlled conditions, the reconstructed facade geometry is sufficiently accurate for facade-scale modeling tasks aimed at recovering wall extents, opening locations, and approximate opening dimensions for renovation-oriented digital documentation or surface estimation. However, these error levels are not claimed to be sufficient for more tolerance-sensitive applications, such as fabrication-ready modeling or detailed installation control, which would require application-specific validation criteria beyond the scope of this study.

Table 1. Runtime breakdown of the proposed pipeline on the synthetic datasets (s)

Dataset	RANSAC	CSG	BIM	Total
Synth0	1830,00	0.06	0.27	1831.33
Synth1	1931,80	0.08	0.25	1932.13
Synth2	2064.29	0.06	0.30	2064.65

The reduction rates remain stable at 96–97%, indicating that only a limited subset of contour points is required for reconstruction. Processing times (Table 1) are almost entirely dominated by the RANSAC-based geometric reconstruction stage, which accounts for about 99.98% of the total runtime. In contrast, CSG and BIM generation contribute negligibly, showing that the main scalability bottleneck lies in geometric fitting rather than IFC-oriented modeling.

4.4 Real PCE results

Four edge detectors were evaluated on the real TLS panoramas: Sobel, Canny, DexiNED, and TEED. Their behavior differs in both contour selectivity and the

Table 2. Quantitative results on synthetic facades. Noise values correspond to Gaussian perturbations.

Dataset	Noise (mm)	PCE red. (%)	Precision	Chamfer (mm)	Hausdorff (mm)	Mean (mm)	Median (mm)	mIoU
Synth0	0	96.81	1.0	0.33	1.35	0.17	0.14	0.999
Synth1	5	96.76	1.0	34.76	72.83	17.38	16.25	0.985
Synth2	10	96.68	1.0	31.78	179.94	15.89	14.55	0.988

number of preserved edge points after reprojection (Table 3). Since the proposed workflow aims to maximize the number of correctly detected structural points for downstream geometric reconstruction, the comparison primarily focuses on true positives. Under this criterion, TEED provides the best overall performance across the two real datasets, with the highest TP count on Lille and one of the highest on Argenteuil. Although it is more sensitive to non-structural edges in cluttered scenes, it most consistently preserves the structural contours needed by the reconstruction stages and was therefore retained as the reference detector.

On the Lille facade, TEED preserves the overall opening layout, with the same recall as GT-PCE (0.93), but lower precision (0.78 vs. 0.98) due to additional non-structural contours. Sobel remains more selective, with higher precision (0.89) but slightly lower recall (0.91), whereas Canny misses many relevant openings (recall 0.48). DexiNED was not retained on Lille because the high number of preserved points after PCE prevented usable downstream reconstruction.

Figure 5. Argenteuil facade : TEED PCE result

The Argenteuil facade is more challenging because numerous fine linear elements, such as cables and facade-mounted equipment, generate strong edge responses that interfere with structural contours. Under the standard opening interpretation, TEED reaches a recall of 0.72 but only a precision of 0.50, which is insufficient for reliable end-to-end reconstruction. Canny provides a better precision-recall balance (0.73-0.72), while Sobel remains lower on both metrics and DexiNED performs poorly.

To further analyze this behavior, a structural (STR) interpretation of openings is introduced for Argenteuil, in which adjacent or double windows are represented by a single enclosing quadrilateral. Under this interpretation, TEED reaches a high recall of 0.94, confirming that the global facade organization is largely preserved despite noise. Precision nevertheless remains low (0.35), showing that the main limitation of automatic PCE lies in its insufficient selectivity toward non-structural facade elements.

Overall, automatic PCE can preserve high structural recall on real facades, but its sensitivity to fine non-structural elements may strongly reduce precision and compromise geometric reconstruction.

4.5 Discussion and limitations

The experiments show that the proposed Scan-to-BIM pipeline depends primarily on the quality and structural consistency of the input edge cloud. While the goal is real-facade reconstruction from TLS data, the geometric stages remain reliable only when extracted contours clearly separate structural from non-structural elements. The real-world evaluation is preliminary and does not support broad claims of robustness or generalizability.

On synthetic datasets, where edge points are derived directly from IFC geometry, the pipeline performs close to ideally. Facade planes, opening boundaries, and corner intersections are reconstructed with limited geometric error, confirming the robustness of the geometric modules when their assumptions are met. These experiments isolate the behavior of the reconstruction stages from acquisition artifacts and edge extraction uncertainty.

On real data, performance is largely governed by the PCE module. On the Lille facade, automatic PCE preserves the dominant window structures and achieves high recall comparable to manually curated PCE, although precision decreases because of spurious contours. Geometric reconstruction nevertheless remains usable. On the Argenteuil facade, fine linear elements such as cables and facade-mounted equipment generate strong edge responses that interfere with window contours. Although automatic PCE still captures the overall facade layout, the resulting edge cloud no longer satisfies the assumptions required for reliable geometric reconstruction. For this reason, the pipeline was stopped after the PCE stage to avoid geometrically misleading results. This case shows that the main limitation of automatic PCE is insufficient selectivity with respect to non-structural elements. Foundation models such as SAM could also be explored

Table 3. Geometric reconstruction results on real-world facades.

Dataset	PCE	Input points	Kept ratio (%)	Runtime (s)	Detected	TP	FN	FP	Duplicates
Lille	GT	56251418	37.87	-	106	104	8	2	1
Lille	Sobel	56251418	14.28	644.46	115	102	10	13	4
Lille	Canny	56251418	7.18	655.10	54	53	58	1	0
Lille	DexiNED	56251418	25.12	897.35	-	-	-	-	-
Lille	TEED	56251418	10.97	907.59	133	104	8	29	9
Argenteuil	GT	143788649	16.16	-	178	178	54	0	0
Argenteuil	Sobel	143788649	7.59	1644.26	217	134	98	83	6
Argenteuil	Canny	143788649	7.51	1597.40	230	168	64	62	24
Argenteuil	DexiNED	143788649	21.0	2542.63	55	8	224	47	0
Argenteuil	TEED	143788649	7.28	2809.34	336	167	65	169	10
Argenteuil (STR)	GT	143788649	16.16	-	178	124	0	54	0
Argenteuil (STR)	TEED	143788649	7.28	2809.34	336	116	8	220	10

as semantic priors, although this is not evaluated in the present study.

The evaluation also does not isolate the error introduced by panoramic projection and reprojection, so the reported metrics reflect the overall pipeline rather than this transformation alone. Overall, the main bottleneck is not geometric reconstruction itself, but the ability of edge extraction to provide structurally valid input. The proposed method should therefore be understood as a semi-automated facade reconstruction workflow rather than a fully automated end-to-end approach.

5 Conclusion

This paper presents a facade Scan-to-BIM pipeline from TLS data combining point cloud edge extraction, geometric reconstruction with simple primitives, and Constructive Solid Geometry (CSG) for BIM-compatible model generation. The proposed framework is semi-automated rather than fully end-to-end, since building isolation remains outside the current operational workflow and the number of facade planes is still specified by the user.

The results show that the geometric reconstruction stages are robust when the input edge cloud preserves a clear structural hierarchy, as confirmed by both synthetic experiments and real-world tests with manually curated PCE. On real-world datasets, however, the main limitation lies in the sensitivity of automatic edge extraction to non-structural facade elements. Although automatic PCE can preserve a high recall of facade structures, its limited selectivity may introduce spurious contours that hinder reliable reconstruction on more complex facades.

Future work should focus on improving the PCE stage, incorporating additional geometric cues, extending validation to a larger set of real facades, and using synthetic data for more controlled training and evaluation of edge extraction. Overall, the main value of this work lies in integrating panoramic edge extraction, interpretable geometric reconstruction, and CSG-based IFC generation into a single facade-oriented workflow, while explicitly identifying both its operating conditions and current failure modes.

6 Acknowledgments

This work was supported by the ByWall project, funded by ADEME.

References

[1] N. Hichri et al. From Point Cloud To BIM: A Survey Of Existing Approaches. *The International Archives of the Photogrammetry, Remote Sensing and Spatial Information Sciences*, pages 343–348, 2013. doi:10.5194/isprsarchives-XL-5-W2-343-2013.

[2] H. Son, C. Kim, and Y. Turkan. Scan-to-BIM - An Overview of the Current State of the Art and a Look Ahead. *ISARC Proceedings*, 2015 Proceedings of the 32nd ISARC, Oulu, Finland:1–8, 2015. doi:10.22260/ISARC2015/0050.

[3] M. Queruel, S. Bornhofen, A. Histace, and L. Ducoulombier. Scan-to-BIM: Unlocking current limitations through Artificial Intelligence. *ISARC Proceedings*, 2024 Proceedings of the 41st ISARC, Lille, France:1040–1047, 2024. doi:10.22260/ISARC2024/0135.

[4] N. Abreu, A. Pinto, A. Matos, and M. Pires. Procedural Point Cloud Modelling in Scan-to-BIM and Scan-vs-BIM Applications: A Review. *ISPRS International Journal of Geo-Information*, 12:260, 2023. doi:10.3390/ijgi12070260.

[5] J. L. Iglesias et al. Revision of Automation Methods for Scan to BIM. In *Advances in Design Engineering*, pages 482–490. Springer International Publishing, 2020. doi:10.1007/978-3-030-41200-5_53.

[6] C. R. Qi, H. Su, K. Mo, and L. J. Guibas. PointNet: Deep Learning on Point Sets for 3D Classification and Segmentation. In *2017 IEEE Conference on Computer Vision and Pattern Recognition (CVPR)*, pages 77–85, 2017. doi:10.1109/CVPR.2017.16.

[7] Y. Wang et al. Dynamic Graph CNN for Learning on Point Clouds. 2019. doi:10.48550/arXiv.1801.07829.

[8] Z. Ding et al. Recent Advances and Perspectives in Deep Learning Techniques for 3D Point Cloud Data Processing. *Robotics*, 12:100, 2023. doi:10.3390/robotics12040100.

[9] S. A. Prieto, E. T. Mengiste, U. Menon, and B. Garcia de Soto. Current State and Trends of Point Cloud Segmentation in Construction Research. *ISARC Proceedings*, 2024 Proceedings of the 41st ISARC, Lille, France:972–979, 2024. doi:10.22260/ISARC2024/0126.

[10] F. Hamid-Lakzaeian and D. F. Laefer. An Integrated Octree-RANSAC Technique for Automated LiDAR Building Data Segmentation for Decorative Buildings. In *Advances in Visual Computing*, pages 454–463. Springer International Publishing, 2016. doi:10.1007/978-3-319-50832-0_44.

[11] B. Yu et al. A Robust Automatic Method to Extract Building Facade Maps from 3D Point Cloud Data. *Remote Sensing*, page 3848, 2022. doi:10.3390/rs14163848.

[12] X. Soria, E. Riba, and A. D. Sappa. Dense Extreme Inception Network: Towards a Robust CNN Model for Edge Detection. In *2020 IEEE Winter Conference on Applications of Computer Vision (WACV)*, pages 1912–1921, 2020. doi:10.1109/WACV45572.2020.9093290.

[13] X. Soria, Y. Li, M. Rouhani, and A. D. Sappa. Tiny and Efficient Model for the Edge Detection Generalization. 2023. doi:10.48550/arXiv.2308.06468.

[14] A. Tabkha, R. Hajji, R. Billen, and F. Poux. Semantic Enrichment of Point Cloud by Automatic Extraction and Enhancement of 360° Panoramas. *The International Archives of the Photogrammetry, Remote Sensing and Spatial Information Sciences*, XLII-2-W17:355–362, 2019. doi:10.5194/isprs-archives-XLII-2-W17-355-2019.

[15] Y. Wang, D. Ewert, D. Schilberg, and S. Jeschke. Edge extraction by merging 3D point cloud and 2D image data. In *2013 10th International Conference and Expo on Emerging Technologies for a Smarter World (CEWIT)*, pages 1–6, 2013. doi:10.1109/CEWIT.2013.6713743.

[16] P. Müller, G. Zeng, P. Wonka, and L. Van Gool. Image-based procedural modeling of facades. *ACM Trans. Graph.*, 26:85–es, 2007. doi:10.1145/1276377.1276484.

[17] C. Yang, T. Han, L. Quan, and C-L. Tai. Parsing façade with rank-one approximation. In *2012 IEEE Conference on Computer Vision and Pattern Recognition*, pages 1720–1727, 2012. doi:10.1109/CVPR.2012.6247867.

[18] C. Dore and M. Murphy. Semi-automatic generation of as-built BIM façade geometry from laser and image data. *Journal of Information Technology in Construction ITCON*, ITcon Vol. 19, pg. 20-46, http://www.itcon.org/2014/2:20–46, 2014.

[19] Q. Wu, K. Xu, and J. Wang. Constructing 3D CSG Models from 3D Raw Point Clouds. *Computer Graphics Forum*, 37:221–232, 2018. doi:10.1111/cgf.13504.

[20] X. Ning, M. Wang, J. Tang, H. Zhang, and Y. Wang. Structural Wall Facade Reconstruction of Scanned Scene in Point Clouds. *Advances in Electrical and Computer Engineering*, 21:11–20, 2021. doi:10.4316/AECE.2021.04002.

[21] S. Boudarbala et al. Automatic detection of doors and windows using point clouds in the context of as-built BIM. *The International Archives of the Photogrammetry, Remote Sensing and Spatial Information Sciences*, XLVIII-2-W8-2024:37–44, 2024. doi:10.5194/isprs-archives-XLVIII-2-W8-2024-37-2024.

[22] X. Hu, Y. Wang, and W. Yu. Image-based laser point cloud building facade structure extraction method by considering semantic information. *npj Herit. Sci.*, 13:160, 2025. doi:10.1038/s40494-025-01728-5.

[23] O. Bohórquez, W Derigent, and H. El Haouzi. Parametric Point Cloud Slicing for Facade Retrofitting. 2021. doi:10.20944/preprints202107.0092.v1.

[24] Dave. D4ve-R/ifcclouds, 2025. URL `https://github.com/D4ve-R/ifcclouds`.